Optimization of an *in vitro* model to study Duchenne Muscular Dystrophy

A Thesis
SUBMITTED TO THE FACULTY OF
UNIVERSITY OF MINNESOTA
BY

Carolina Ortiz Cordero

IN PARTIAL FULFILLMENT OF THE REQUIREMENTS
FOR THE DEGREE OF
MASTER OF SCIENCE

Rita Perlingeiro

December, 2014

Acknowledgements

I would like to express my gratitude to Dr. Perlingeiro for the invaluable opportunity, her guidance, patient and willingness to help. Furthermore I would like to thank Dr. Keirstead for the useful comments and engagement through the process of this master. I would like to thank all the Perlingeiro Lab members for their inspiring guidance, irreplaceable constructive criticism and friendly advice throughout the research. I would finally like to thank my family for their unquestionable support and encouragement.

Table of Contents

List of Tables

List of Figures

Introduction

Skeletal muscle is one of the main tissues found in the mammalian body, playing a role in producing body movement, stabilizing the body position, storing and moving substances and producing heat. To do so muscle cells are electrically excitable, have the ability to contract when stimulated, are extensible and elastic. Two key features that allow these unique functions are the sarcolemma and the sarcoplasmic reticulum (SR). The sarcolemma, the cell membrane of the muscle fibers, has invaginations that tunnel through the fibers from the outside towards the center called transversel tubules (T-tubules). The T-tubules are adjacent on both sides to the ends of the SR (terminal cisternae), a specialized endoplasmic reticulum that stores calcium ions when the muscle cells are relaxed (**Fig. 1.**). When the muscle is electrically stimulated action potentials propagate through the T-Tubules causing the activation of the voltage-dependent calcium channels, which trigger the opening of ryanodine receptors in the SR surrounding myofibers. This allows the release of calcium and contraction of the fibers (Totora & Derrickson, 2009). As a result of the emptying of the stores, the store operated calcium entry (SOCE) will be activated allowing Ca^{+2} from the extracellular matrix to come into the cells. Simultaneously the Sarco/endoplasmic Reticulum Ca2+-ATPase (SERCA) will pump calcium ions back into the SR. Thus the sarcolemma plays a fundamental role in the propagation of action potentials needed for contraction. Additionally the sarcolemma has an essential role in the capacity of the cells to withstand the strain caused by contraction of the fibers. When the

sarcolemma is unstable affected muscle can give rise to a muscle disease. One key gene that has been associated with membrane stability is the dystrophin gene (DMD).

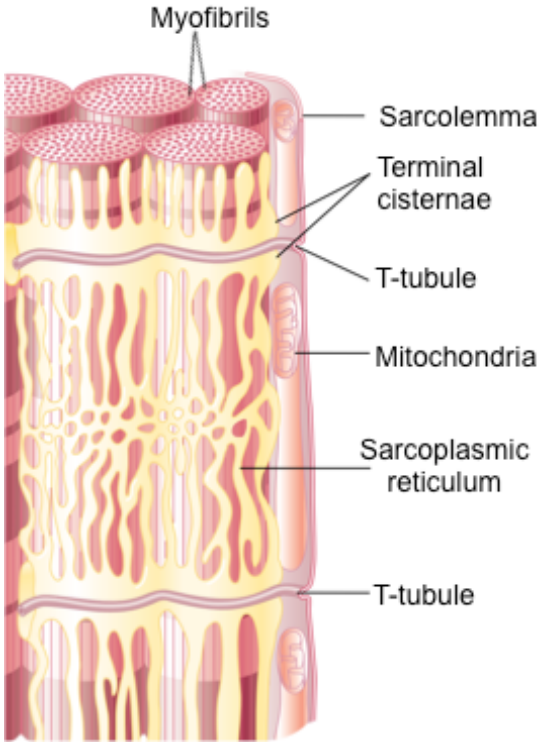

Figure 1. Sarcolemma-sarcoplasmic reticulum system. Transverse tubules (T-tubule) from the sarcolemma surround the myofiber. The sarcoplasmic reticulum terminal cisternae are adjacent to both sides of the T-tubules. Modified from Guyton & Hall (2006).

DMD gene, Dystrophin and associated proteins

The dystrophin gene, is located in chromosome X, is composed of 79 exons and encodes the longest known primary transcript in the human genome. Full-length

dystrophin has at least 4 promoters and several internal promoters that generate 4 shorter isoforms. Additionally the gene encodes circular RNA and long non-coding RNA (Blake et al., 2002; Bovolenta et al., 2012; Surono et al., 1999). The DMD gene has been found to be mainly expressed in skeletal and cardiac muscle, but it is also found in the brain (Blake et al., 2002).

The DMD gene encodes for Dystrophin, a 427kDa cytoskeletal protein with a rod shape located in the cytoplasmic side of the sarcolemma that stabilizes the membrane by linking the actin and intermediate filaments with transmembrane complexes. Dystrophin consists of 4 domains: the actin-binding domain, the central rod-like domain, the cysteine-rich domain and the C-terminal domain (Muntoni et al., 2003). Dystrophin forms part of the dystrophin-associated glycoprotein complex (DGC) a transmembrane complex, which links the sarcolemma and the extracellular matrix. DGC is involved in membrane stabilization, force transmission, synapse formation and molecular signaling (Pilgram et al., 2010). Members of the DGC include dystrobrevins (DTNA), syntrophins (α1, β1, β2, γ1, and γ2), dystroglycan (DG-α/β), sarcoglycans (SG-α, SG-β, SG-γ, SG-δ, SG-ε, and SG- ζ), neuronal nitric oxide synthase (nNOS) and sarcospan (SSPN). Dystrophin's cysteine-rich domains interacts directly with DG-β, which spans the cell membrane and interacts with DG-α that binds agrin and laminin in the extracellular matrix (**Fig. 2**; Pilgram et al., 2010). The C-terminal domain interacts with dystrobrevins and syntrophins. Additionally the large central rod interacts with nNOS (Nigro & Piluso, 2014). When dystrophin is

absent, the DGC complex is unstable or mislocalized, disrupting the mechanical and signaling functions of the complex, causing Duchenne Muscular Dystrophy.

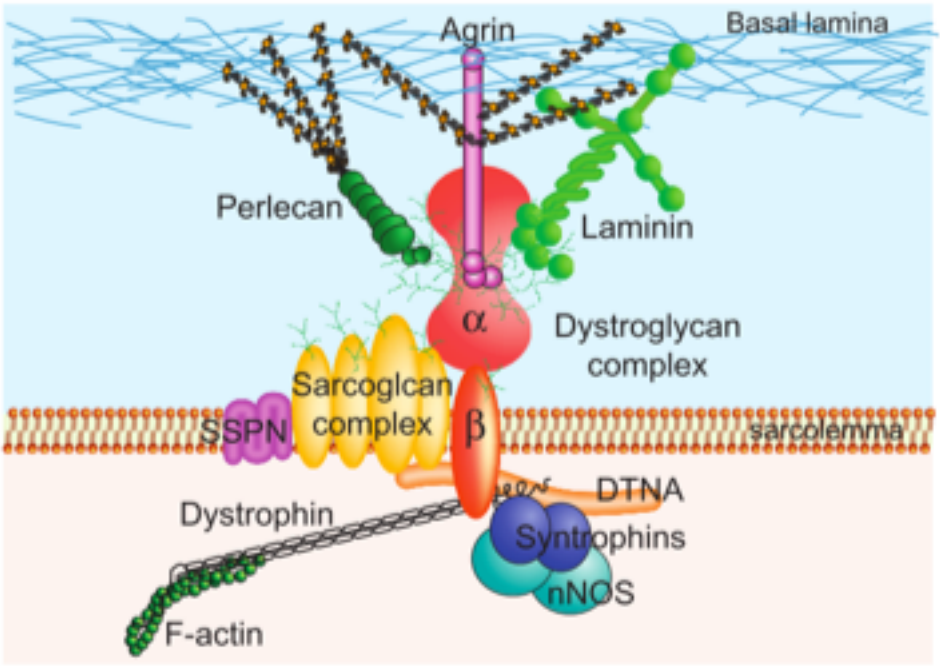

Figure 2. Dystrophin-associated glycoprotein complex. Dystrophin links dystroglycan with the sub sarcolemma protein F-actin. Extracted from Kobayashi & Campbell (2012).

Duchenne Muscular Dystrophy

Duchenne Muscular Dystrophy (DMD) is the most common inherited muscular dystrophy affecting 1:5000 male live births (Bushby et al., 2010). DMD is characterized by progressive muscle wasting of skeletal and cardiac muscle. In the early phase of the disease, skeletal muscles of DMD patients presents an ongoing process of degeneration and regeneration, which is later, followed by

exhaustion of regenerative capacity, fibrosis, and eventual disruption of the muscle tissue architecture. Clinically, DMD patients experience progressive muscle weakness and atrophy, and are confined to a wheelchair before the age of 12 with eventual death due to respiratory and/or cardiac failure. Although DMD has been extensively studied, to date there are no effective therapies.

DMD pathology results from genetic and biochemical defects in the dystrophin-glycoprotein complex caused by mutations in the DMD gene. In DMD, no functional dystrophin protein is produced while in Becker muscular dystrophy (BMD), a milder form, the mutation generates a truncated dystrophin protein. There are a variety of mutations associated with DMD; exon deletion accounts for approximately 60-70% of mutations and can comprise one or more exons. These mutations are mainly located at the 3' of the gene (exons 44–53) and at the 5' (exons 3–19). Small deletions or insertions, single-base changes and splicing mutations account for nearly 25–35% of mutations. Large duplications account for 5–10 % of mutations and approximately 2 % are thought to be intronic rearrangements or 5′ and 3′UTR changes (Wang et al., 2014).

Pathophysiology in DMD skeletal muscle

Sarcolemma instability has been proposed as one of the main pathological features of DMD. Using the tracer molecule Evans blue, it was observed that skeletal muscle fibers from mouse carrying a spontaneous mutation in the DMD

gene (known as mdx) accumulate this dye, whereas there is no accumulation in skeletal muscle fibers of normal mice. This indicates that the dystrophin mutation disrupts the plasma membrane (Straub et al., 1997). Additionally the release of cell enzymes, like creatine kinase, into the circulation have been documented as one of the initial clinical manifestations of DMD (Swaiman & Sandier, 1963; Blake et al., 2002). Consistently these observations are amplified when mice were subjected to exercise, which causes increased muscle degeneration (Brussee et al., 1997). Moreover when muscles from mice have been prevented from contracting by immobilization, denervation or treatment with tetanus toxin, no DMD phenotype has been observed (Karpati et al., 1988; Mariol et. al., 2007; Mizuno, 1992), further indicating the role of physical strain on the muscle as a hallmark for degeneration.

Abnormal calcium homeostasis has been observed in muscle lacking functional dystrophin. An increase in Ca+2 concentration in the cytosol and increased Ca2+ uptake by the mitochondria has been documented in resting and stimulated skeletal muscle of mdx (Pertille et. al., 2010; Turner et al., 1991) and DMD patients (Bertorini et al., 1982; Imbert et al., 2001; Mongini et al., 1988). Furthermore increased calcium influx activates proteases that lead to necrosis, which potentiates the degeneration/regeneration observed in DMD (Pertille et al., 2010). As disease progresses there is a decline in regeneration capacity leading to increased connective and adipose tissue in the muscles. A role for dystrophin in this process has been proven by overexpression of dystrophin in mdx mice,

which was able to restore Ca+2 levels, suggesting a relation between DGC destabilization and irregular calcium homeostasis (Denetclaw et al., 1994).

Millay et al. (2009) and Goonasekera et al. (2014) showed that increased SOCE is sufficient in mice to develop a DMD-like phenotype in mice. SOCE is activated once the sarcoplasmic reticulum calcium stores are empty, allowing the entry of extracellular calcium. Two main types of channels have been suggested to be involved; the TRPC family and the STIM1/Orai1 complex (**Fig. 3**), although a clear mechanism has not been established (Kiviluoto et al., 2011). Overexpression of STIM1 (Goonasekera et al., 2014) or TRPC3 (Millay et al., 2009) in two independent studies led to an increase in cytosolic Ca+2 concentration and to myofiber degeneration/regeneration, necrosis and fibrosis. Moreover the inhibition of Ca2+ influx diminished the dystrophic phenotypes (Goonasekera et al., 2014; Millay et al., 2009). Consistently, TRPC1 and STIM1/Orai1 have been found up-regulated in mdx mice (Edwards et al., 2010; C. Vandebrouck et al., 2002). Importantly a recent study has found TRPC1 to be up regulated in DMD patient biopsies (Kiviluoto et al., 2011). Additionally, co-immunoprecipitation studies have shown that TRPC1 binds syntrophin and forms a complex with dystrophin in skeletal muscle (A. Vandebrouck et al., 2007). Thus it appears that when the DGC complex is disrupted, TRPC1 mediates increased Ca+2 entry (Sabourin et al., 2009). All these studies demonstrate the hallmarks of the disease, although to date, a clear understanding of the pathophysiology behind DMD remains elusive.

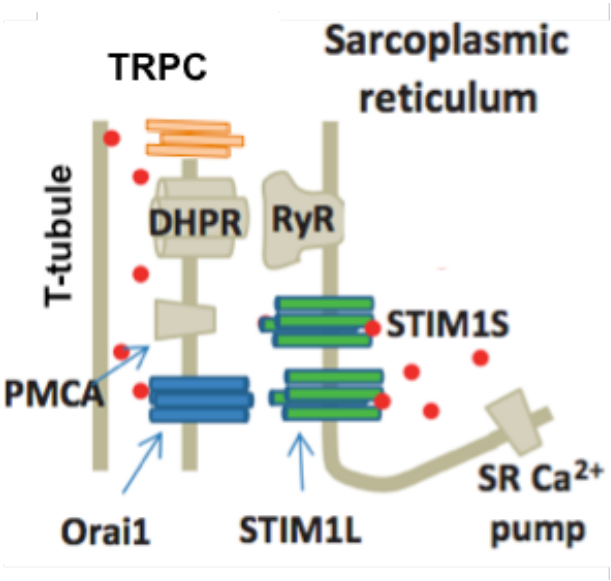

Figure 3. Proposed channels involved in SOCE. Channels are located in the SR terminal cisternae and neighbor t-tubule. DHPR, dihydropyridine receptor; RyR, ryanodine receptor; PMCA, plasma membrane Ca2+-ATPase; STIM1S, stromal interaction molecule 1 short; STIM1L, stromal interaction molecule 1 long. Modified from Cully & Launikonis (2013).

In vitro DMD model

Mouse models have been reported to display a DMD phenotype. Although mdx mice have been widely used this model displays a milder phenotype due to the up-regulation of utrophin, a substitute of dystrophin more commonly expressed during development (Helliwell et al., 1992; Love et al., 1989). The mdx mouse displays decrease force but this weakness does not present until older age and there is no change in lifespan. The dystrophin/utrophin double knockout (dKO)

displays a more severe phenotype characterized by a marked muscular dystrophy that results in reduced life span (Deconinck et al., 1997). Nevertheless neither model is suitable to recapitulate DMD pathogenesis.

The technology of reprogramming somatic cells to induce pluripotent stem cells (iPS) offers an unlimited source of material, allowing later differentiation into diverse tissue types, opening the possibility to further investigate *in vitro* disease modeling. Adult somatic cells from DMD patients have been subjected to reprogramming by introducing the pluripotency factors (Oct4, Sox2, KLF4; Takahashi et al., 2007), and the resulting induced pluripotent stem (iPS) cells have been differentiated into muscle progenitor cells using the conditional expression of Pax7 (Darabi et al., 2012). This approach allows for the *in vitro* generation of large quantities of early embryonic skeletal myogenic progenitors in mouse and human cells (Darabi et al., 2011 & 2012). Furthermore transplantation of these cells into dystrophic mice results in myofiber and satellite cell engraftment that is accompanied by improvement in muscle force generation (Darabi et al. 2012; Filareto et al., 2013). As expected based on the in vivo results, myocytes derived from human embryonic stem cells (ES) and iPS cells showed electrophysiological properties typical for mammalian skeletal muscle. Both cell types displayed the sarcomeric organization found in skeletal muscle as well as the excitation contraction coupling machinery. Of note, the authors concluded these muscle preparations were not physiologically mature in culture due the observation of a high variability in the slow component of the intracellular

calcium decay (Skoglund et al., 2014).

Based on previous studies showing the capacity to generate iPS derived myocytes, we aim to establish an *in vitro* model using iPS DMD derived myocytes. This approach presents a non-invasive and renewable platform to further study the pathophysiology of the disease. Using iPS cells derived from patients with DMD, we aspire to determine if a DMD phenotype can be detectable *in vitro.* To do so, we generated iPS-cell derived mature skeletal muscle fibers, and measured the capacity of these fibers to respond to depolarization induced by high potassium. We also studied gene expression of proteins involved in the excitation of the muscle fibers. Additionally, by measuring intracellular calcium concentration, we hypothesized that DMD and control fibers, would have similar intracellular calcium concentrations and SOCE when the cells have not been stimulated.

Materials and Methods

Generation of myogenic progenitors from ES and iPS cell lines

Previous studies in the laboratory showed that Pax7, a paired box transcription factor required for satellite cell maintenance, could efficiently induce the myogenic program of differentiating ES and iPS cells (Darabi et al., 2011). Inducible Pax7 iPS cell line from a DMD patient with a mutation causing the loss of exons 52 to 54 and human control Pax7 H9 ES cells were generated as before (Darabi et al., 2012). After confirming stable expression of Pax7, cells were differentiated as embryoid bodies (EBs). Cells were expanded in the absence of Dox in T25 flasks. Confluent (75%) cells were collected using Accumax (Millipore) and then plated in 60x15mm low adherent Petri dishes containing 5ml mTeSR media and 10μM ROCK inhibitor. Dishes were placed in an orbital shaker (60RPM) in an incubator and after 2 days media, that was substituted with 5ml of myogenic induction media consisted of Iscove's Modified Dulbecco's Medium (Gibco) containing 15% fetal bovine serum (Gibco), 10% horse serum (Sigma), 1% chick embryo extract (US Biological), 50μg/ml ascorbic acid (Sigma), 4.5 mM monothioglycerol, and 10 μM ROCK inhibitor (for 24 hours), and kept on the shaker for 5 more days. Afterwards EBs were collected by gravity and plated in T75 flasks coated with gelatin in the presence of myogenic media supplemented with 5ng/ml bFGF (R&D). Three days after plating EBs as monolayers, media was replaced with myogenic media containing

dox (0.75µg/ml) and 5ng/ml bFGF and grown for 4 more days. Cells were then harvested from flasks using Trypsin, and sorted for mCherry+ (Pax7+) cells. After sorting Pax7 positive cells (p0) were plated in gelatin coated T25 flask at the density of 40000-50000/cm2 in the same myogenic medium supplemented with Dox and human bFGF (5ng/ml; **Fig. 4 a-b I-II-III**).

Differentiation of myogenic progenitors to myocytes

Confluent cultures of p2-p3 myogenic cells were harvested using Trypsin and plated on gelatinized glass coverslips (22x22, 1.5 thickness) at 6,000 cells/cm2-12,000 cells/cm2 with the same myogenic proliferation media. Media was replaced every other day, and once cells were confluent, the media was substituted with differentiation media consisting of low glucose DMEM containing 2% (vol/vol) horse serum and 1% insulin–transferrin–selenium (Gibco; **Fig. 4b IV-V**).

iPax3 Satellite Cells

Previous members in the Perlingeiro laboratory isolated satellite cells from 6-8 week-old Pax7-ZsGreen/mdx or R26-M2rtTA/M2rtTA;Pax7-ZsGreen mice as described previously (Bosnakovski et al., 2008), and transduced with the inducible Pax3/IRES mCherry lentiviral vector (Filareto et al., 2013) to generate the iPax3-satellite cells and mdx-iPax3-satellite cells

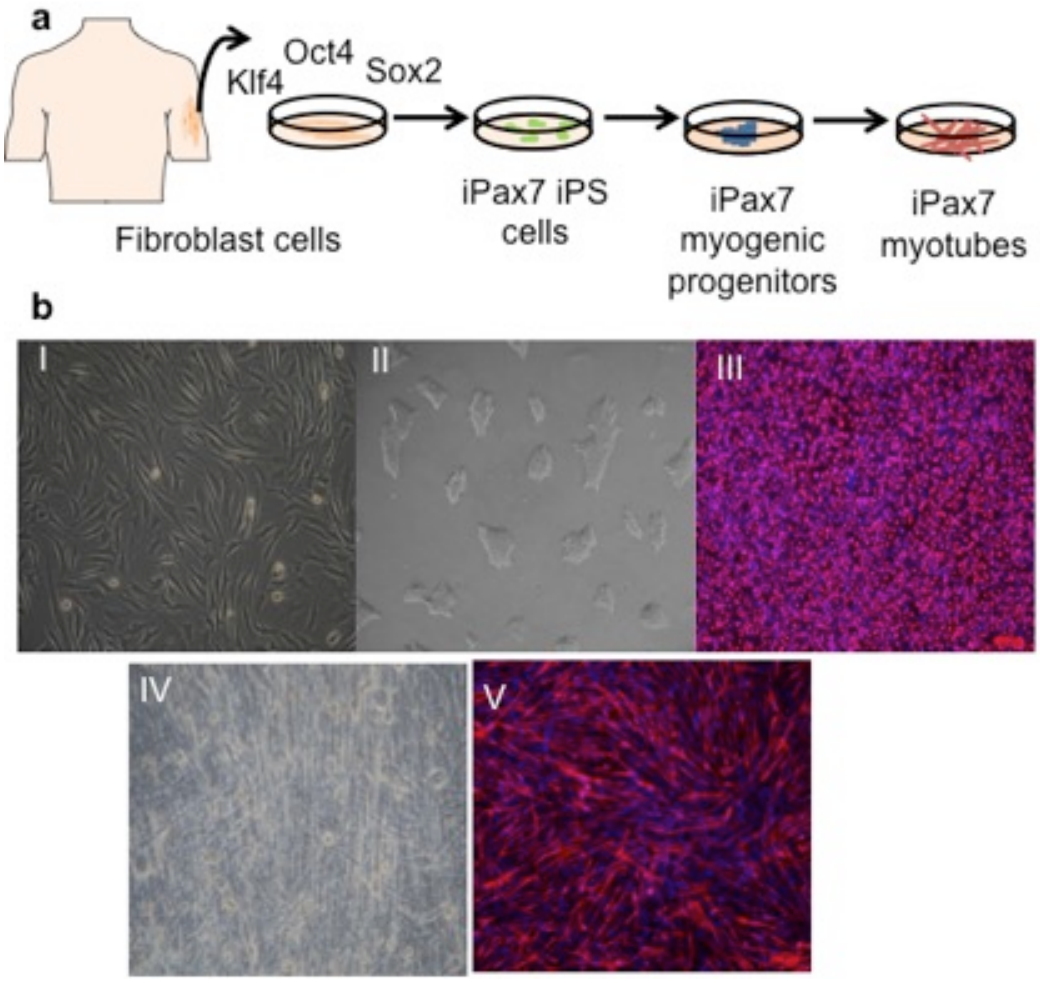

Figure 4. From skin to myotubes. (a) Schematic representation of the steps involved in myotube derivation. (b) Representative images of (I) fibroblasts obtained from a DMD patient, which were subjected to reprogramming by introducing the pluripotency factors (Oct4, Sox2, KLF4) to generate patient-specific iPS cells (II). These cells were engineered as described into proliferating myogenic progenitors (III). Pax 7 expression is shown in red and nuclei in blue. In the presence of low serum containing medium, progenitor cells differentiate into myotubes (IV), as shown by the expression MHC in red (V). Nuclei are shown in blue.

Immunofluorescence staining

Cells plated on 22x22 cm coverslips were fixed with 4% PFA or methanol (human Dystrophin staining). After 10 minutes PFA was removed and cells were permeabilized with 0.03% Triton X-100 (Sigma) in PBS. Cells were blocked with 3% bovine serum albumin (BSA) in PBS for 1 hour and then incubated with the primary antibody overnight. Before incubating in the secondary antibody, cells were washed twice with PBS. DAPI (1:5000) was used for nuclei staining. Specific information about the antibodies is listed in Table 1.

Calcium imaging

To assess DMD iPS-derived myocytes, calcium levels were measured in cells that had differentiated for 3-8 weeks on coverslips. The changes in intracellular calcium were measured using Fura-2 AM, a ratiometric fluorescent calcium indicator. Cells were loaded with fura-2/AM for 1 hour at room temperature in standard control Ringer solution (pH7.4). Once loaded, cells were placed in a perfusion chamber mounted on an inverted epifluorecense microscope with a galvanometric wavelength switcher. Cells were continuously superfused at a rate of 2ml per minute using a four way manual valve and analyzed 20 minutes afterwards with a 40x oil immersion objective. Loaded cells were maintained in control Ringer solution for 240s and then perfused for 40s with high potassium (50mM) calcium-free Ringer solution to assess the E/C coupling of the cells (**Fig.**

5). Afterwards cells were rinsed with control Ringer solution for 240s. Once intracellular calcium levels returned to baseline, cells were perfused for 120s with calcium free Ringer solution. To promote depletion of sarcoplasmic reticulum calcium store, cells were submitted to 120s of perfusion with the SERCA inhibitor thapsigargin (2μM) in calcium-free Ringer solution. To further empty calcium from the sarcoplasmic reticulum, cells were perfused with 10mM caffeine plus 2μM thapsigargin in zero calcium Ringer solution for 120s. Finally to demonstrate store operated calcium entry, the cells were perfused for 120s with control Ringer solution. Due to the heterogeneity of the population, only cells that displayed a response to depolarization were analyzed. Acquisition and analysis were performed using MetaFluor.

Western Blott

Proteins from cell preparations were isolated using Radioimmunoprecipitation assay buffer (RIPA buffer) supplemented with protease inhibitor (Sigma). 50 ng of protein were separated on 8% SDS-polyacrylamide gel, transferred to a nitrocellulose membrane and probed with primary antibodies **(Table 1)**. Protein levels were quantified using ImageJ, by comparing sample bands to control bands.

Fig 5. Calcium imaging experimental scheme. Differentiated myocytes pre-loaded for 1 hour with Fura 2-AM were maintained in control Ringer solution (CR) for 180s and then perfused for 60s with potassium solution (50mM; HiK). Afterwards cells were rinsed with CR for 240s. Once intracellular calcium levels returned to baseline, cells were perfused for 120s with calcium free Ringer solution (0CaCR). To promote depletion of sSR calcium store, cells were submitted to 120s of perfusion with the SERCA inhibitor thapsigargin (2μM) in calcium-free Ringer solution (+Thap). To further empty calcium from the SR, cells were placed in 10mM caffeine with 2μM thapsigsrgin in zero calcium Ringer solution for 120s (+Caff). Finally to promote the activation of SOCE the cells will be perfused for 120s with control Ringer solution (CR). Gray filled areas denote the solution had calcium.

RT-PCR

RNA was isolated using a PureLink RNA Mini kit (Life technologies), RNA was further purified using DNase 1 (Invitrogen) and reverse-transcribed using Thermo Script RT-PCR System (Invitrogen) according to manufacturers' protocols. Quantitative RT–PCR was performed in duplicates using the Biomark 96.96 Dynamic Array system (Fluidigm) using TaqMan Gene Expression Assays (Applied Biosystems).

Table 1. Antibodies and dilutions used for immunofluorescence and western blot

Primary Antibody	**Provider**	**Dilution**	**Secondary Antibody**	**Provider**	**Dilution**
Myosin heavy Chain	DSHB	1:20	Alexa Fluor 555 Goat anti Mouse	Invitrogen	1:400
Dystrophin	Abcam	1:250	Alexa Fluor 555 Goat anti Rabbit	Invitrogen	1:400
Myogenin	DSHB	1:200	Alexa Fluor 555 Goat anti Mouse	Invitrogen	1:400
TRPC1	Sigma	1:200	Amersham WB goat anti-rabbit Cy5	GE	1:5000
Actin			Amersham WB mouse anti-rabbit Cy5	GE	1:5000

Statistics

Statistical analyses of the data obtained were performed by the Student t-test for comparison between two samples with a normal distribution. The non-parametric Mann-Whitney Test was used for samples that did not have a Gaussian distribution. To determine which test to use D'Angostino-Pearson omnibus normality test was performed. All calculations were done using Prism 6 (GraphPad Software Inc.). The error bars in all the graphs represent the standard deviation (SD).

Results

Generation of ES/iPS derived myocytes

Control H9 and DMD iPS-derived myogenic progenitors were generated as described in Materials and Methods. Myocytes with typical elongated morphology emerged in these cultures. To confirm mature myogenic identity, we performed immunofluorescence. Both cell types gave rise to myogenin and MHC positive fibers. As expected no dystrophin expression was found in DMD iPS-derived myocytes (**Fig 6**).

Ca2+ Measurement and SOCE Activity

As shown in Fig. 7 we were able to detect changes in intracellular calcium concentration. To establish a system to determine if increased calcium concentration, a hallmark of DMD phenotype, was observable after electric pulse stimulation we first quantified intracellular calcium concentration using Fura 2 in un-stimulated cells. Both cell types had fibers that responded to excitation by high extracellular potassium with an increase in calcium concentration (**Fig. 8**). Control H9 myocytes had a higher variability in the magnitude of response to increased potassium concentration and in basal calcium levels than DMD iPS-derived myocytes (**Fig. 9**).

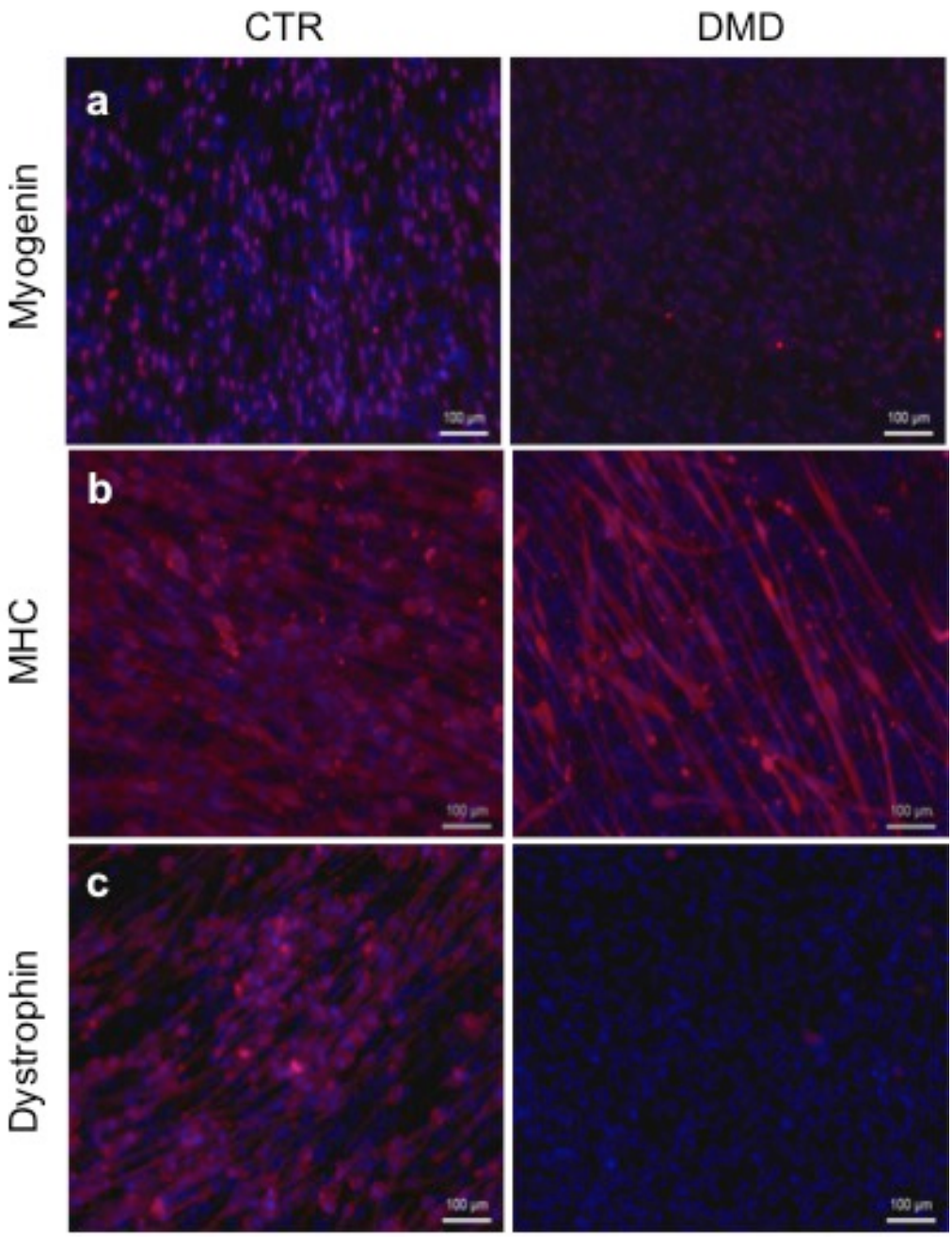

Figure 6. Human myocytes express markers of late myogenesis Immunohistochemistry for myogenin (a), MHC (b) and dystrophin (c) in red of control H9 or DMD iPS-derived myocytes after 54 and 25 days in differentiation respectively. Nuclei in blue.

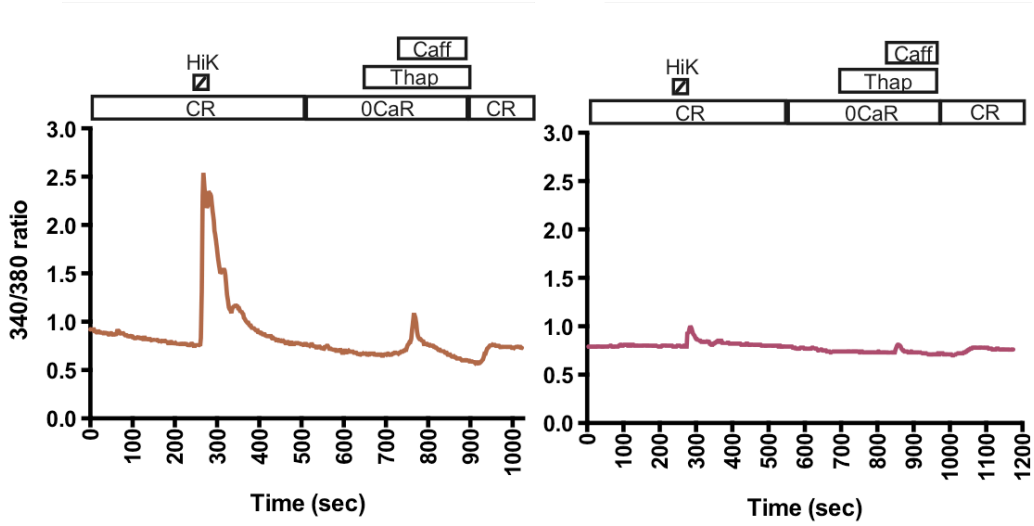

Figure 7. Control H9 cells have a higher change in intracellular calcium in response to stimuli than DMD iPS-derived myocytes. Representative Fura 2 AM traces of control H9 myocytes 28 days post differentiated (a) and 35 days differentiated DMD iPS-derived myocytes (b).

Basal calcium levels were comparable between the two groups (**Fig. 8a**). Due to the variability observed in response to depolarizing the membrane using increased extracellular potassium we decided to consider responses only in fibers that had an increased in calcium, due to depolarization, higher than 0.2. DMD iPS-derived fibers had increased basal intracellular calcium concentration (**Fig. 8b**; $p<0.05$) while the control H9 cells had an increased response to high potassium and to SOCE (**Fig. 8c & 8d;** $p<0.01$). Although the cells were grown under the same conditions there was a high degree of variability in basal calcium and in the magnitude of response to depolarization among experiments for both cell lines (**Fig. 9**). Consequently, a relationship between the basal calcium by

days of differentiation with response to high potassium or SOCE could not be determined.

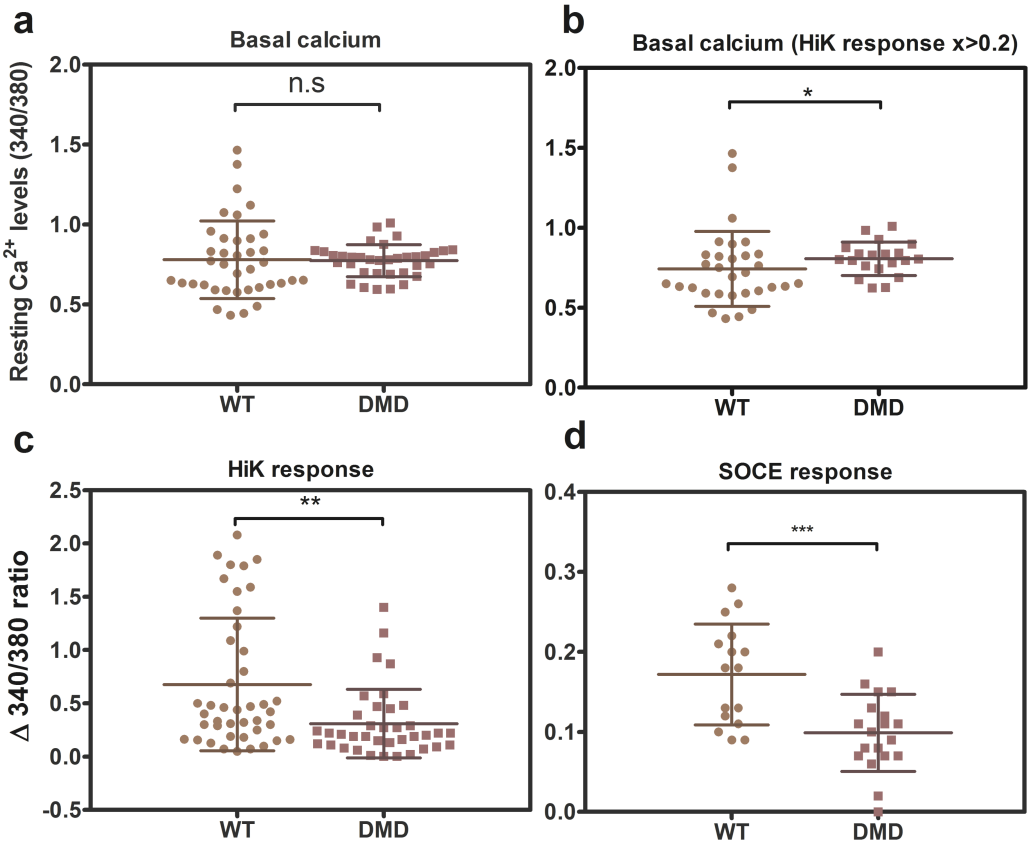

Figure 8. Control H9 myocytes display increased levels of intracellular calcium in response to induced depolarization and SOCE. Quantitation of multiple traces for basal calcium in all the cells (a), basal calcium for fibers with change in calcium free high potassium (50mM) superior to 0.2 (b), response to high potassium (50mM) (c) and store operated calcium entry (d) for H9 control myocytes (WT) and iPS-derived myocytes from a DMD patient. To determine changes in the above parameters variations in Fura 2 AM ratio were quantified. Measurements were obtained from 4 different experiments. n.s >0.05, * p<0.05, ** p<0.001. Whiskers represent standard deviation. See also Fig. 5.

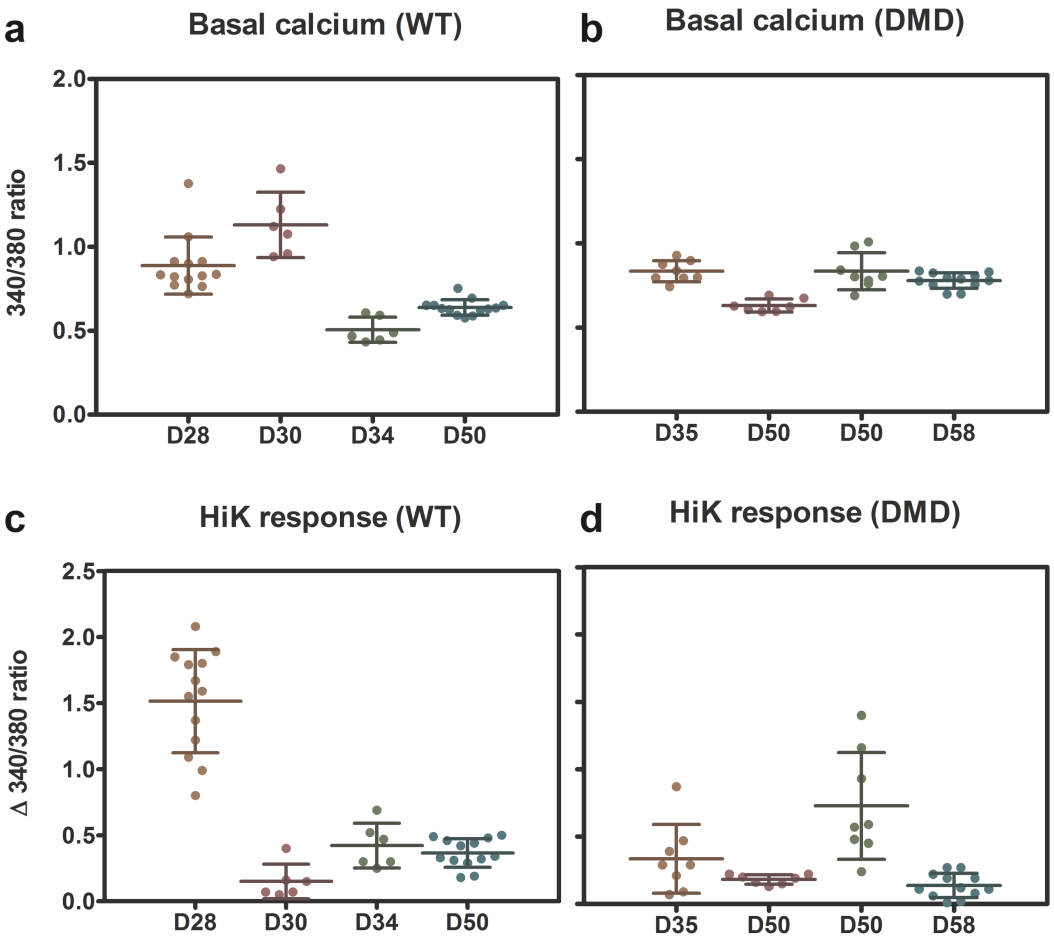

Figure 9. Basal calcium and response to high potassium induce excitation varies between experiments. Quantitation of basal calcium and high potassium (50mM) for Control H9 (WT) and DMD iPS-derived myocytes at different times of differentiation for 4 different experiments. Whiskers represent standard deviation.

Expression of channels and receptors involved in excitation/contraction coupling in human cell lines

In another set of experiments we evaluated by quantitative PCR expression levels of channels and receptors involved in the excitation/contraction coupling of the sarcolemma. We chose to study ryanodine receptors, type 1 and 3 (RyR); L-type calcium channel Alpha (CACNA) 1C and 1S Subunits; the sarco/endoplasmic Reticulum Ca2+-ATPase 2 (ATP2) subunit a2 and a1; and Type IV and V Sodium Channel, Voltage-Gated Alpha Subunit (SCN4A and SCN5A). Expression levels in Control H9 and DMD iPS derived myocytes were compared with myocytes differentiated from myoblast isolated from primary tissue. Myocytes from healthy individuals tended to expressed more RYR1 than RyR3 and more CACNA1S than CACNA1C. RyR3 is typically more related to muscle in development then RyR1. While CACNA1S is more commonly found in skeletal muscle versus CACNA1C that is generally associated with cardiac muscle. As for DMD derived myocytes expression levels of RyR and CACNA were very low **(Fig. 10a-b)**. ATP2a2 had higher levels in all cell lines than ATP2a1, suggesting that the cells tend to be mostly of slow twitch muscle fibers (**Fig. 10c**). Additionally the expression levels of SCN5A tended to be higher in the healthy samples versus DMD iPS-derived samples in which SCN4A was higher (**Fig. 10d**).

Additionally transient receptor potential cation channel 1 (TRPC), a channel involved in SOCE, has been associated with the DMD phenotype. No statistically

significant differences were found between Control H9 and the DMD iPS-derived lines by quantitative PCR or western blot. This may be due to the variability in the level of maturation of the preparations (**Fig. 11**).

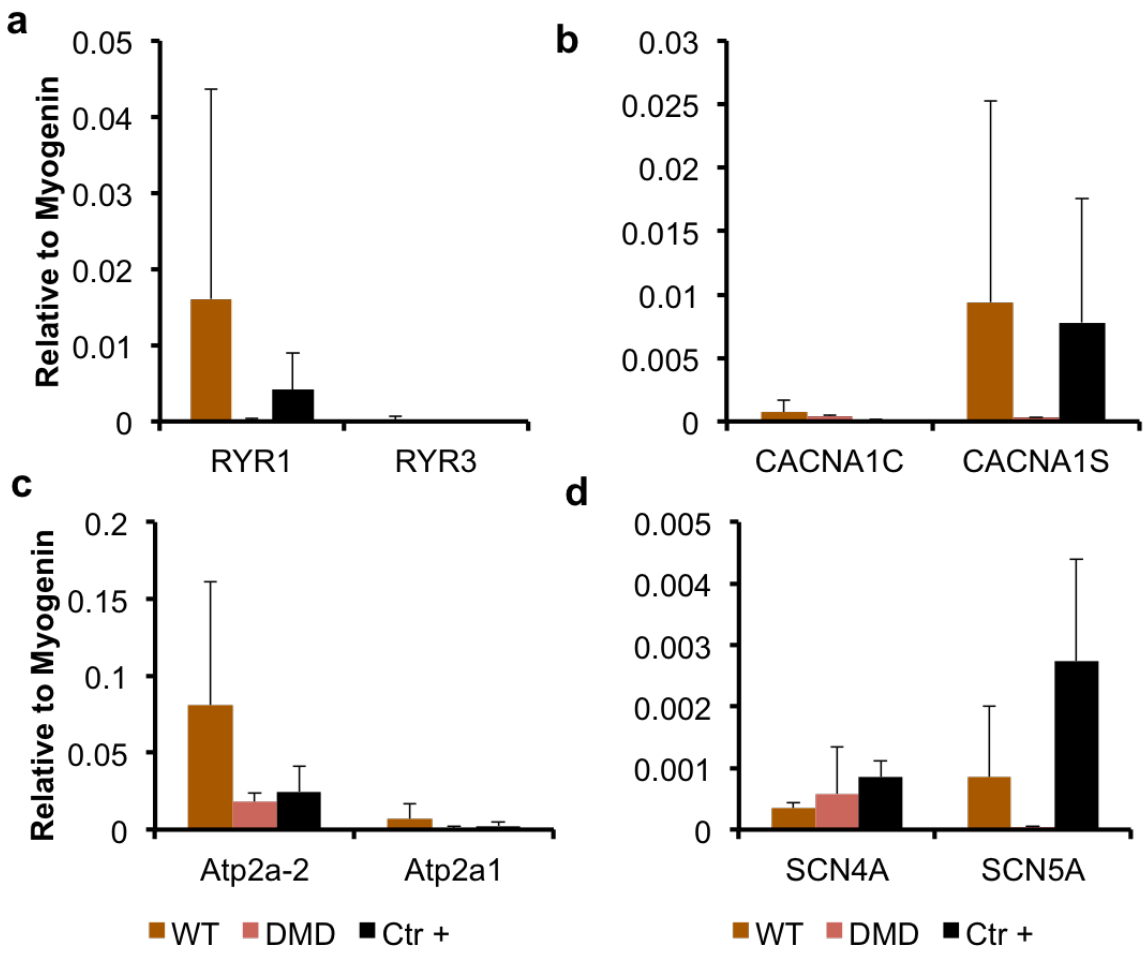

Figure 10. Expression of channels and receptors involved in muscle contraction. Quantitative PCR for Ryanodine Receptor Type 1 and 3 (a); Calcium Channel, Voltage-Dependent, L Type, Alpha 1C and 1S Subunit (b); Sarco/endoplasmic Reticulum Ca2+-ATPase Subunit 2a 1 and 2 (c) and Sodium Channel, Voltage-Gated, Type IV and V, Alpha Subunit (d) for Control H9 (WT) and DMD iPS-derived myocytes (DMD) after 40 days of differentiation. Error bars represent SD from three independent experiments.

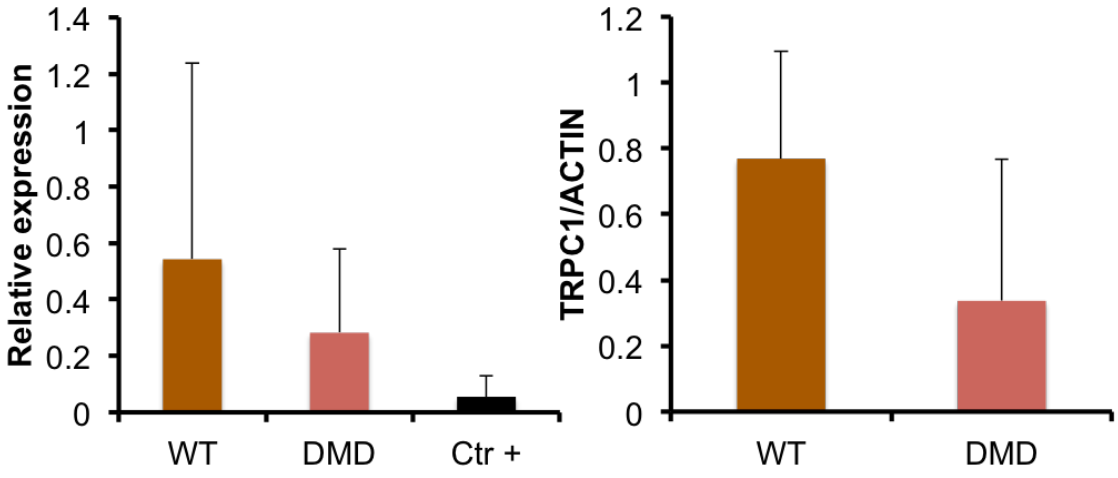

Figure 11. TRPC levels in Control H9 and DMD iPS-derived myocytes vary. Relative expression of mRNA by quantitative PCR (a) and inmmunoblotting (b) for TRPC1 at 40 days of differentiation for ES derived H9 myocytes and iPS Duchenne Muscular Dystrophy derived 1705 myocytes. Expression levels were normalized to Myogenin and ACTIN respectively. TRPC1 is shown relative to wild type (WT) in right panel. Bars represent SD for two replicates of three independent experiments (left) and two independent experiments (right).

Mouse iPax3 Satellite Cell derived myocytes

Because of the high variability observed with these early findings involving human ES/iPS derived myogenic progenitors, we decided to investigate whether a DMD phenotype could be observed in an *in vitro* system with less variability. Previously isolated and modified iPax3 Satellite cells from wild type and mdx mice were differentiated for 4 days. Both cells types generated MYOG and MHC positive fibers (**Fig. 12**).

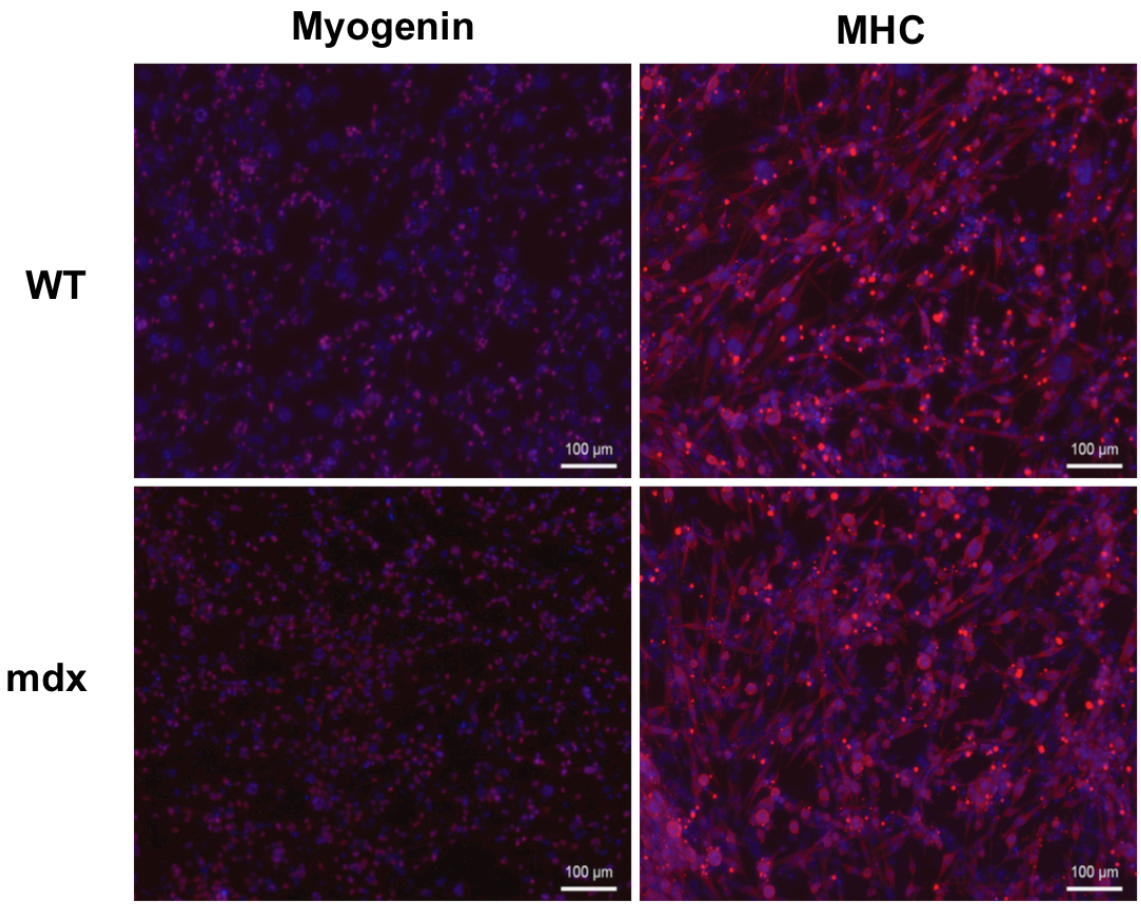

Figure 12. iPax3 mouse Satellite cells differentiate into myocytes. Immunohistochemistry for myogenin **(a)** and MHC **(b)** in red for wild type (WT) and mdx myocytes 4 days post differentiation. Nuclei in blue.

Using the same conditions as in human cells, we measured intracellular calcium for the mouse wild type and mdx satellite cell derived myocytes. As before, we were able to quantify changes in intracellular calcium concentration in both cell lines (**Fig. 13**). Wt and mdx muscle fibers responded to depolarization induced by high extracellular potassium. Additionally both cell lines had equal

concentration of basal calcium under normal conditions. Consistent with the observations in human myocytes, wild type mouse myocytes had a higher increase in intracellular calcium when the membrane was depolarized by high concentration of extracellular potassium then mdx derived myocytes. Unlike the human cells, both mdx and WT mouse cell lines had similar increases in calcium concentration due to SOCE (**Fig. 14**). In general mouse iPax3 satellite cell derived myocytes had a higher change in calcium concentration and a smaller range of response for both depolarization and SOCE than human myocytes.

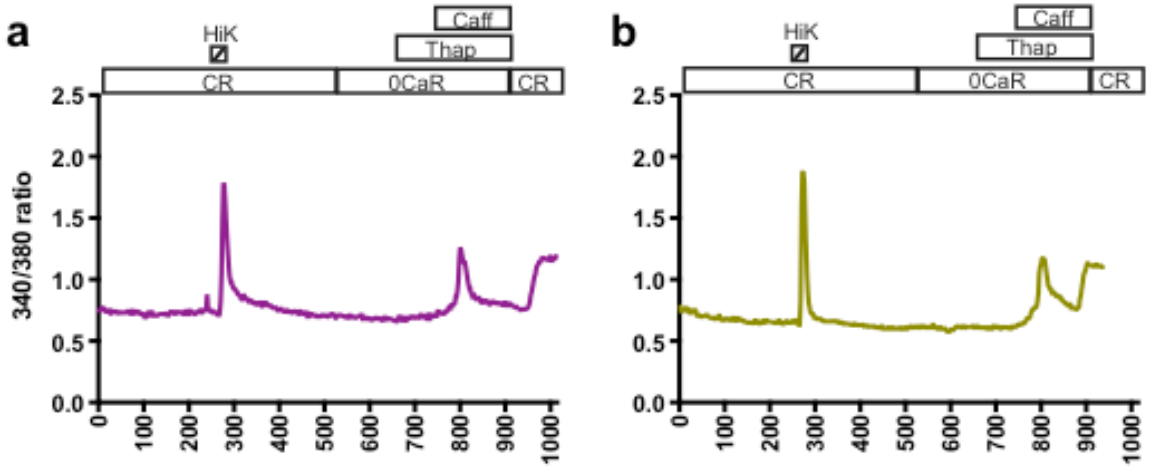

Figure 13. Myotubes derived from wt and mdx mice have similar responses to external stimuli. Representative Fura 2 traces of satellite cell derived myotubes from wild type mice (a), and mdx pax3 mice (b). Calcium levels were measured at 7 and 4 days respectively.

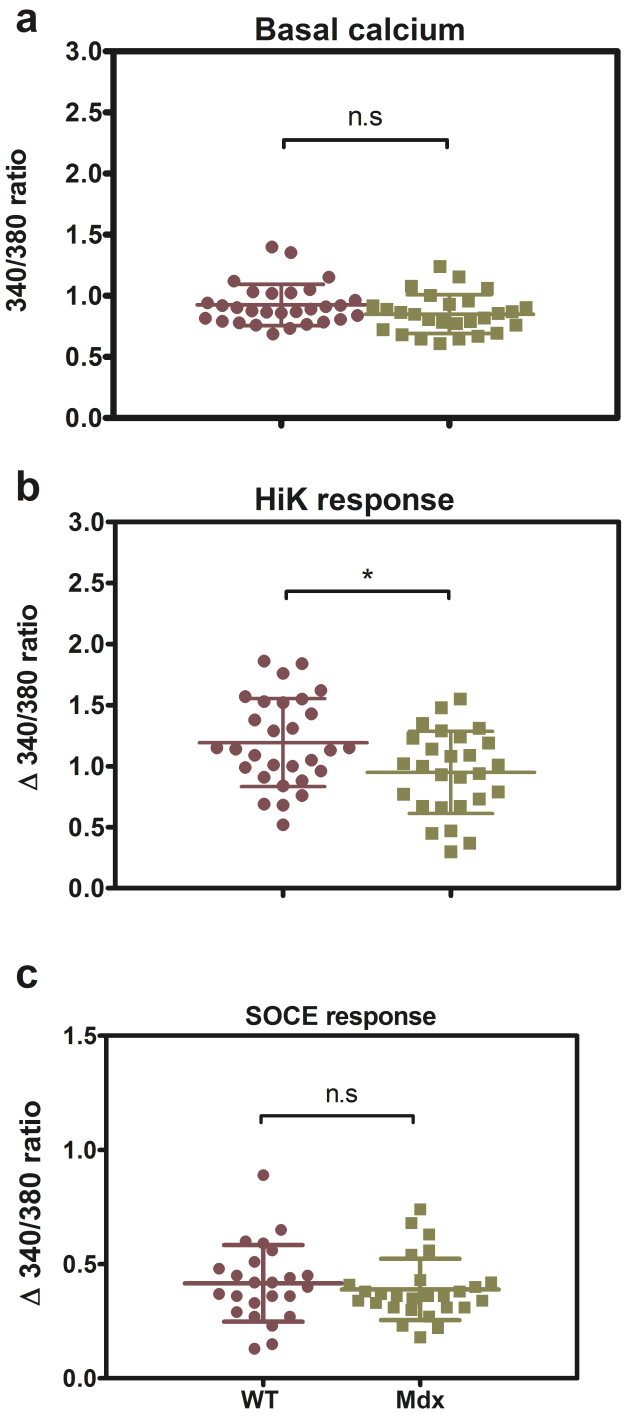

Figure 14. Myotubes derived from wt and mdx mice have similar basal calcium levels. Quantitation of multiple traces for basal calcium **(a)**, response to high potassium (50mM) **(b)** and store operated calcium entry **(c)** for satellite cell derived myocytes from wild type mice (WT) and mdx Pax3 mice (mdx) at 7 and 4 days respectively. To determine changes in the above parameters in Fura 2 AM ratio were quantified. Measurements were obtained from 1 experiment. n.s >0.05, * p<0.05. Whiskers represent standard deviation. See also Fig 11.

Discussion

Duchenne Muscular dystrophy is a complex disease to which a clear pathophysiology remains elusive. Due to the difficulties to obtain primary muscle from DMD patients, generating a comprehensive *in vitro* model is consequential. Using the protocol previously established (Darabi et al., 2008, 2011, 2012) we were able to recapitulate myogenesis and generate myogenin and MHC positive fibers from human ES/iPS derived myogenic progenitors *in vitro*. Both these proteins are late markers of myogenesis. Despite this, the population of cells had different degrees of maturation, exemplified by the variability in the change in the intracellular calcium concentration observed when cells were depolarized by increased extracellular potassium suggests that there is a heterogeneous population. Cseri and collaborators (2002) observed in human and mouse skeletal muscle cultures that potassium failed to elicit a change in calcium concentration in myoblasts, but as fibers were more mature, (determined by the number of nuclei) the change in calcium concentration increased. Although a response to potassium was used as a reference to identify mature fibers, different levels of maturity may be found in the selected population, reflected by the wide range of response to depolarization. DMD iPS-derived myocytes seemed to display a lower degree of maturation. Previous studies have determined that both ES and iPS derived myocytes have similar electrophysiological properties, although both were considered to be immature (Skoglund et al., 2014). Essential channels and receptors necessary for

membrane depolarization and excitation-contraction coupling seem to be expressed at low levels and to a varying degree in the differentiated cells. This variability is consistent with the different levels of maturation observed in the calcium analysis. A limitation of current techniques to assess gene expression and protein levels is that quantitative PCR and Western blot measure the total RNA and protein in the entire population, so unless the population only contains myocytes and the fibers have a similar degree of maturation the results will reflect the cumulative levels of the cells which can easily be influenced by extreme values.

Due to the high level of variability in the human ES/iPS derived myocytes we decided to test if differences in the physiology could be observed *in vitro* using modified satellite cells isolated from wild type and mdx mice. Satellite cells are stem cells of the muscle involved in giving rise to myogenic progenitor cells and mediate growth, maintenance and regeneration of skeletal muscle (Yin, Price, & Rudnicki, 2013). As satellite cells are already committed to the myogenic lineage we expected that differentiation into myocytes would be more homogeneous than the human ES/iPS-derived myocytes. As expected, un-stimulated fibers, had comparable basal calcium and SOCE (Karpati et al., 1988; Mariol et al. 2007). Although further repetitions are necessary to determine the reproducibility of the results, we validate that these cells can be used to generate a consistent system. Future experiments will aim to determine if a DMD phenotype is observed when electric pulses stimulate the cells to induce damage. This can be assayed by calcium concentration analysis and other membrane permeability assays.

Due to the high variability of maturation observed in the cultured ES/iPS derived human myocytes, a phenotype for DMD could not be clearly established. One major goal is to establish a robust system to ensure the majority of the cells reach the same level of myogenic maturation. One possible approach to solve this issue is the transfection of the ES/iPS cells with MyoD before inducing differentiation. Furthermore ES/iPS cells can be co-cultured with motorneurons that may assist in maturation of fibers. An additional point to address would be the establishment of a system to determine clearly which cells have the highest level of maturity. Once a robust basal system is established, the future goal will be to recapitulate the DMD associated pathology in these cells to further understand intrinsic aspects of the dystrophy. This could provide an *in vitro* model for drug discovery.

Bibliography

Bertorini, T. E., Bhattacharya, S. K., Palmieri, G. M. A., Chesney, C. M., Pifer, D., & Baker, B. (1982). Muscle calcium and magnesium content in Duchenne muscular dystrophy. *Neurology*, *32*(April 1982), 1088–1092.

Blake, D. J., Weir, A., Newey, S. E., & Davies, K. A. Y. E. (2002). Function and Genetics of Dystrophin and Dystrophin-Related Proteins in Muscle. *The Americal Phisiology Society*, *82*, 291–329.

Bosnakovski, D., Xu, Z., Li, W., Thet, S., Cleaver, O., Perlingeiro, R. C. R., & Kyba, M. (2008). Prospective isolation of skeletal muscle stem cells with a Pax7 reporter. *Stem Cells (Dayton, Ohio)*, *26*(12), 3194–204. doi:10.1634/stemcells.2007-1017

Bovolenta, M., Erriquez, D., Valli, E., Brioschi, S., Scotton, C., Neri, M., … Ferlini, A. (2012). The DMD locus harbours multiple long non-coding RNAs which orchestrate and control transcription of muscle dystrophin mRNA isoforms. *PloS One*, *7*(9), e45328. doi:10.1371/journal.pone.0045328

Brussee, V., Tardif, F., & Tremblay, J. P. (1997). Muscle fibers of mdx mice are more vulnerable to exercise than those of normal mice. *Neuromuscular Disorders : NMD*, *7*(8), 487–92.

Bushby, K., Finkel, R., Birnkrant, D. J., Case, L. E., Clemens, P. R., Cripe, L., … Constantin, C. (2010). Diagnosis and management of Duchenne muscular dystrophy, part 1: diagnosis, and pharmacological and psychosocial management. *Lancet Neurology*, *9*(1), 77–93. doi:10.1016/S1474-4422(09)70271-6

Cseri, J., Szappanos, H., Szigeti, G. P., Csernátony, Z., Kovács, L., & Csernoch, L. (2002). A purinergic signal transduction pathway in mammalian skeletal muscle cells in culture. *Pflügers Archiv : European Journal of Physiology*, *443*(5-6), 731–8. doi:10.1007/s00424-001-0757-x

Darabi, R., Arpke, R. W., Irion, S., Dimos, J. T., Grskovic, M., Kyba, M., … Michael Kyba, R. C. R. P. (2012). Human ES- and iPS-derived myogenic progenitors restore DYSTROPHIN and improve contractility upon transplantation in dystrophic mice. *Cell Stem Cell*, *10*(5), 610–9. doi:10.1016/j.stem.2012.02.015

Darabi, R., Arpke, R. W., Irion, S., Dimos, J. T., Grskovic, M., Kyba, M., & Perlingeiro, R. C. R. (2012a). Human ES- and iPS-derived myogenic progenitors restore DYSTROPHIN and improve contractility upon

transplantation in dystrophic mice. *Cell Stem Cell*, *10*(5), 610–9. doi:10.1016/j.stem.2012.02.015

Darabi, R., Arpke, R. W., Irion, S., Dimos, J. T., Grskovic, M., Kyba, M., & Perlingeiro, R. C. R. (2012b). Supplemental Information Human ES- and iPS-Derived Myogenic Progenitors Restore Dystrophin and Improve Contractility upon Transplantation in Dystrophic Mice Figure S1 . iPS Cell Production , generation of inducible PAX7 pluripotent cells and myogenic indu, *10*, 1–19.

Darabi, R., Gehlbach, K., Bachoo, R. M., Kamath, S., Osawa, M., Kamm, K. E., … Perlingeiro, R. C. R. (2008). Functional skeletal muscle regeneration from differentiating embryonic stem cells. *Nature Medicine*, *14*(2), 134–43. doi:10.1038/nm1705

Darabi, R., Santos, F. N. C., Filareto, A., Pan, W., Koene, R., Rudnicki, M. A., … Perlingeiro, R. C. R. (2011). Assessment of the Myogenic Stem Cell Compartment Following Transplantation of Pax3/Pax7 -Induced Embryonic Stem Cell-Derived Progenitors. *Stem Cells*, *29*(5), 777–790. doi:10.1002/stem.625.Assessment

Deconinck, A. E., Rafael, J. A., Skinner, J. A., Brown, S. C., Potter, A. C., Metzinger, L., … Holloway, R. (1997). Utrophin-Dystrophin-Deficient Mice as a Model for Duchenne Muscular Dystrophy. *Cell*, *90*, 717–727.

Denetclaw, W. F., Hopf, F. W., Cox, G. a, Chamberlain, J. S., & Steinhardt, R. a. (1994). Myotubes from transgenic mdx mice expressing full-length dystrophin show normal calcium regulation. *Molecular Biology of the Cell*, *5*(10), 1159–67.

Edwards, J. N., Friedrich, O., Cully, T. R., von Wegner, F., Murphy, R. M., & Launikonis, B. S. (2010). Upregulation of store-operated Ca2+ entry in dystrophic mdx mouse muscle. *American Journal of Physiology. Cell Physiology*, *299*(1), C42–50. doi:10.1152/ajpcell.00524.2009

Filareto, A., Parker, S., Darabi, R., Borges, L., Iacovino, M., Schaaf, T., … Perlingeiro, R. C. R. (2013). An ex vivo gene therapy approach to treat muscular dystrophy using inducible pluripotent stem cells. *Nature Communications*, *4*, 1549. doi:10.1038/ncomms2550

Goonasekera, S. a, Davis, J., Kwong, J. Q., Accornero, F., Wei-LaPierre, L., Sargent, M. a, … Molkentin, J. D. (2014). Enhanced Ca^{2+} influx from STIM1-Orai1 induces muscle pathology in mouse models of muscular dystrophy. *Human Molecular Genetics*, *23*(14), 3706–15. doi:10.1093/hmg/ddu079

Helliwell, T. R., Man, N. T., E., M. G., & Davies, K. E. (1992). The Dystrophin-Related Protein, Utrophin, Is Expressed On The Sarcolemma Of Regenerating Human Skeletal Muscle Fibres In Dystrophies And Inflammatory Myopathies. *Neuromuscular Disorders*, *2*(3), 177–184.

Imbert, N., Vandebrouck, C., Duport, G., Raymond, G., Hassoni, a a, Constantin, B., … Cognard, C. (2001). Calcium currents and transients in co-cultured contracting normal and Duchenne muscular dystrophy human myotubes. *The Journal of Physiology*, *534*(Pt. 2), 343–55.

Karpati, G., Carpenter, S., & Prescott, S. (1988). Small-Caliber Skeletal Muscle Fibers Do Not Suffer Necrosis In Mdx Mouse Dystrophy. *Muscle & Nerve*, *11*, 795–803.

Kiviluoto, S., Decuypere, J.-P., De Smedt, H., Missiaen, L., Parys, J. B., & Bultynck, G. (2011). STIM1 as a key regulator for Ca2+ homeostasis in skeletal-muscle development and function. *Skeletal Muscle*, *1*(1), 16. doi:10.1186/2044-5040-1-16

Kobayashi, Y. M., & Campbell, K. P. (2012). Skeletal Muscle Dystrophin-Glycoprotein Complex and Muscular Dystrophy. In *Muscle: Fundamental Biology and Mechanisms of Disease* (First Edit., pp. 935–942). Elsevier Inc. doi:10.1016/B978-0-12-381510-1.00066-1

Love, D. R., Hill, D. F., Dickson, G., Spurr, N. K., Byth, B. C., Marsden, R. F., … Davies, K. E. (1989). An autosomal transcript in skeletal muscle with homology to dystrophin. *Nature*, *339*, 55–58.

Mariol, M.-C., Martin, E., Chambonnier, L., & Ségalat, L. (2007). Dystrophin-dependent muscle degeneration requires a fully functional contractile machinery to occur in C. elegans. *Neuromuscular Disorders : NMD*, *17*(1), 56–60. doi:10.1016/j.nmd.2006.09.012

Millay, D. P., Goonasekera, S. a, Sargent, M. a, Maillet, M., Aronow, B. J., & Molkentin, J. D. (2009). Calcium influx is sufficient to induce muscular dystrophy through a TRPC-dependent mechanism. *Proceedings of the National Academy of Sciences of the United States of America*, *106*(45), 19023–8. doi:10.1073/pnas.0906591106

Mizuno, Y. (1992). Prevention of myonecrosis in mdx mice: Effect of immobilization by the local tetanus method. *Brain and Development*, *14*(5), 319–322. doi:10.1016/S0387-7604(12)80151-3

Mongini, T., Ghigo, D., Doriguzzi, C., Bussolino, F., Pescarmona, G., & Pollo, B. (1988). Free cytoplasmic Ca ++ at rest and after cholinergic stimulus is

increased in cultured muscle cells from Duchenne muscular dystrophy patients. *Neurology*, *38*(April 1987), 476–480.

Muntoni, F., Torelli, S., & Ferlini, A. (2003). Review Dystrophin and mutations : one gene , several proteins , multiple phenotypes. *The Lancet Neurology*, *44*(0), 731–740.

Nigro, V., & Piluso, G. (2014). Spectrum of muscular dystrophies associated with sarcolemmal-protein genetic defects. *Biochimica et Biophysica Acta*. doi:10.1016/j.bbadis.2014.07.023

Pertille, A., de Carvalho, C. L. T., Matsumura, C. Y., Neto, H. S., & Marques, M. J. (2010). Calcium-binding proteins in skeletal muscles of the mdx mice: potential role in the pathogenesis of Duchenne muscular dystrophy. *International Journal of Experimental Pathology*, *91*(1), 63–71. doi:10.1111/j.1365-2613.2009.00688.x

Pilgram, G. S. K., Potikanond, S., Baines, R. a, Fradkin, L. G., & Noordermeer, J. N. (2010). The roles of the dystrophin-associated glycoprotein complex at the synapse. *Molecular Neurobiology*, *41*(1), 1–21. doi:10.1007/s12035-009-8089-5

Sabourin, J., Lamiche, C., Vandebrouck, A., Magaud, C., Rivet, J., Cognard, C., … Constantin, B. (2009). Regulation of TRPC1 and TRPC4 cation channels requires an alpha1-syntrophin-dependent complex in skeletal mouse myotubes. *The Journal of Biological Chemistry*, *284*(52), 36248–61. doi:10.1074/jbc.M109.012872

Skoglund, G., Lainé, J., Darabi, R., Fournier, E., Perlingeiro, R., & Tabti, N. (2014). Physiological and ultrastructural features of human induced pluripotent and embryonic stem cell-derived skeletal myocytes *in vitro*. *Proceedings of the National Academy of Sciences of the United States of America*, *111*(22), 8275–80. doi:10.1073/pnas.1322258111

Straub, V., Rafael, J. a., Chamberlain, J. S., & Campbell, K. P. (1997). Animal Models for Muscular Dystrophy Show Different Patterns of Sarcolemmal Disruption. *The Journal of Cell Biology*, *139*(2), 375–385. doi:10.1083/jcb.139.2.375

Surono, A., Takeshima, Y., Wibawa, T., Ikezawa, M., Nonaka, I., & Matsuo, M. (1999). Circular dystrophin RNAs consisting of exons that were skipped by alternative splicing. *Human Molecular Genetics*, *8*(3), 493–500.

Swaiman, K. F., & Sandier, B. (1963). The use of serum creatine phosphokinase and other serum enzymes in the diagnosis of progressive muscular dystrophy. *The Journal of Pediatrics*, *63*(6), 1116–1119.

Takahashi, K., Tanabe, K., Ohnuki, M., Narita, M., Ichisaka, T., Tomoda, K., & Yamanaka, S. (2007). Induction of pluripotent stem cells from adult human fibroblasts by defined factors. *Cell*, *131*(5), 861–72. doi:10.1016/j.cell.2007.11.019

Turner, P. R., Fong, P. Y., Denetclaw, W. F., & Steinhardt, R. a. (1991). Increased calcium influx in dystrophic muscle. *The Journal of Cell Biology*, *115*(6), 1701–12.

Vandebrouck, A., Sabourin, J., Rivet, J., Balghi, H., Sebille, S., Kitzis, A., … Constantin, B. (2007). Regulation of capacitative calcium entries by alpha1-syntrophin: association of TRPC1 with dystrophin complex and the PDZ domain of alpha1-syntrophin. *FASEB Journal : Official Publication of the Federation of American Societies for Experimental Biology*, *21*(2), 608–17. doi:10.1096/fj.06-6683com

Vandebrouck, C., Martin, D., Colson-Van Schoor, M., Debaix, H., & Gailly, P. (2002). Involvement of TRPC in the abnormal calcium influx observed in dystrophic (mdx) mouse skeletal muscle fibers. *The Journal of Cell Biology*, *158*(6), 1089–96. doi:10.1083/jcb.200203091

Wang, Y., Yang, Y., Liu, J., Chen, X.-C., Liu, X., Wang, C.-Z., & He, X.-Y. (2014). Whole dystrophin gene analysis by next-generation sequencing: a comprehensive genetic diagnosis of Duchenne and Becker muscular dystrophy. *Molecular Genetics and Genomics : MGG*. doi:10.1007/s00438-014-0847-z

Yin, H., Price, F., & Rudnicki, M. a. (2013). Satellite cells and the muscle stem cell niche. *Physiological Reviews*, *93*(1), 23–67. doi:10.1152/physrev.00043.2011